IMMUNOLOGY

High-throughput functional screening for next-generation cancer immunotherapy using droplet-based microfluidics

Yuan Wang[1†], Ruina Jin[1†], Bingqing Shen[2], Na Li[1], He Zhou[2], Wei Wang[3], Yingjie Zhao[4,5], Mengshi Huang[2], Pan Fang[2], Shanshan Wang[2], Pascaline Mary[2], Ruikun Wang[1], Peixiang Ma[3], Ruonan Li[1], Yujie Tian[1], Youjia Cao[1], Fubin Li[4,5], Liang Schweizer[2], Hongkai Zhang[1,3]*

Currently, high-throughput approaches are lacking in the isolation of antibodies with functional readouts beyond simple binding. This situation has impeded the next generation of cancer immunotherapeutics, such as bispecific T cell engager (BiTE) antibodies or agonist antibodies against costimulatory receptors, from reaching their full potential. Here, we developed a highly efficient droplet-based microfluidic platform combining a lentivirus transduction system that enables functional screening of millions of antibodies to identify potential hits with desired functionalities. To showcase the capacity of this system, functional antibodies for CD40 agonism with low frequency (<0.02%) were identified with two rounds of screening. Furthermore, the versatility of the system was demonstrated by combining an anti-Her2 × anti-CD3 BiTE antibody library with functional screening, which enabled efficient identification of active anti-Her2 × anti-CD3 BiTE antibodies. The platform could revolutionize next-generation cancer immunotherapy drug development and advance medical research.

INTRODUCTION

Cancer immunotherapies that harness the power of the immune system to treat tumors have brought great progress and driven a major paradigm shift in cancer treatment. The first generations of cancer immunotherapy agents consist primarily of antagonist antibodies that block negative immune checkpoints, such as programmed cell death protein 1 (PD-1) (*1*–*3*). Recently, next-generation cancer immunotherapies, including bi/multispecific antibodies, such as bispecific T cell engager (BiTE) antibodies and agonist antibodies of costimulatory receptors, have been claiming the spotlight, showing promise in triggering anticancer immunity (*4*–*7*).

In vitro display technology, such as phage display, allows the selection of antibody binders from large combinatorial libraries with a capacity of 10^{11} diversities (*8*–*13*). This has been one of the major technologies in conventional antibody drug development through the use of high- or low-throughput simple binding assays.

Next-generation cancer immunotherapies, including agonist or bi/multispecific antibodies, have yet to fulfill their full potential. This may be, at least in part, due to the low throughput of functional screens (maximally, a few thousand antibodies can be tested), representing a bottleneck that requires prescreens to narrow down potential candidates and may cause loss of certain target profiles, depending on the criteria set for the prescreens. In addition, bi/multispecific antibody development may also suffer from a lack of diversity driven by limited candidate generations using validated monospecific antibodies with known bispecific scaffolds.

Droplet microfluidic technology allows analysis and screening of cells at the single-cell level with unprecedented throughput, something that cannot be obtained using bulk population-based assays. The microfluidic droplet system can encapsulate single cells in water-in-oil droplets at a rate of thousands of droplets per second (*14*). Antibodies generated by the cells are contained in the droplet, enabling the maintenance of phenotype and genotype linkage within the droplet (*15*–*17*). Last, droplets containing desirable cells are sorted by fluorescence-activated droplet sorting (FADS). El Debs *et al.* and Shembekar *et al.* (*18*, *19*) described application of the microfluidic droplet system for screening hundreds of thousands of hybridoma cells for antibodies that inhibit enzyme angiotensin-converting enzyme 1 (ACE-1) or bind to target cells (*18*, *19*). With the sophistication of the microfluidic droplet system, simultaneous analyses of millions of individual antibody-secreting plasma cells for their antibody secretion rate and affinity can be achieved (*20*). Millions of plasma cells can be screened for antibodies bound to vaccines or cancer targets (*21*). However, improvement is urgently needed to screen for functional antibodies.

Here, we developed an efficient technology platform to simultaneously screen for the binding and agonistic activity of antibodies or the functions of bispecific antibodies. This approach combines the strength of an autocrine-based lentiviral transduction system with the microfluidic droplet system (*22*–*26*). The technical capabilities of the platform were demonstrated by the successful identification of rare potent costimulatory receptor CD40 agonist antibodies and active anti-Her2 × anti-CD3 bispecific antibodies from a combinatorial antibody library. This streamlined technology enables efficient and unbiased discovery of active antibodies with markedly increased throughput and accuracy to serve as the next generation of cancer immunotherapy.

[1]State Key Laboratory of Medicinal Chemical Biology and College of Life Sciences, Nankai University, Tianjin, China. [2]HiFiBiO (Shanghai) Co. Ltd., Shanghai, China. [3]Shanghai Institute for Advanced Immunochemical Studies, ShanghaiTech University, Shanghai, China. [4]Shanghai Institute of Immunology, Faculty of Basic Medicine, Shanghai Jiao Tong University School of Medicine, Shanghai, China. [5]Key Laboratory of Cell Differentiation and Apoptosis of Chinese Ministry of Education, Shanghai Jiao Tong University School of Medicine, Shanghai, China.
*Corresponding author. Email: hongkai@nankai.edu.cn
†These authors contributed equally to this work.

RESULTS

Outline of function-based antibody selection using droplet-based microfluidics

We designed the functional antibody selection platform as depicted in Fig. 1. Cells were infected by a lentiviral antibody-expressing library at a multiplicity of infections (MOI) equal to 1 so that each cell expressed and secreted only one type of antibody. For microfluidic-based screening, individual antibody-secreting cells were coencapsulated with a reporter cell into a droplet by a microfluidic drop maker. The resulting emulsion was incubated off-chip overnight and injected into the sorting chip. Droplets containing activated reporter cells were sorted by FADS. Subsequently, cells were recovered from the droplets, and functional antibodies were identified by sequencing the antibody genes in the sorted cells.

Development and optimization of droplet-based assay

Two microfluidic devices were used (i) to compartmentalize the lentivirus-infected cells with reporter cells and detection reagents (Fig. 2, A and B) and (ii) to sort droplets based on reporter cell activation and receptor binding signals using a surface acoustic wave–based sorter (Fig. 2C) (*27*). The throughput of the microfluidic device for droplet formation and sorting is on the order of millions of droplets within hours per instrument.

Droplets generated by the microfluidic chip were incubated for 24 hours at 37°C. No merging of droplets was observed, indicating that the droplets were stable (Fig. 2B). Next, we used an anti-Her2 × anti-CD3 BiTE antibody as an example for the development and optimization of the droplet-based assay. The anti-Her2 × anti-CD3 BiTE positive control was engineered to recognize Her2 on tumor cells and CD3 on T cells using the variable domain sequences of trastuzumab and blinatumomab, respectively (*28*). Her2-overexpressing K562-Her2 cells were infected with the anti-Her2 × anti-CD3 BiTE positive control lentivirus at a low MOI, resulting in less than 10% of cells being infected. K562-Her2 played a dual role in expressing antibodies and providing Her2-mediated cross-linking of the secreted antibodies. Each infected K562-Her2 cell was encapsulated with a Jurkat/pIL2–enhanced green fluorescent protein (eGFP) reporter cell (fig. S1, A and B) with 0.5 antibody-secreting cells and 1 reporter cell per droplet on average. The number of cells per droplet was analyzed on the basis of the fluorescent signal from the antibody-secreting cell labeled with CellTrace Violet dye and the reporter cell labeled with CellTrace Yellow dye. The results were in good agreement with the theoretical double Poisson distribution, with 4524 droplets analyzed (fig. S2). After 16 hours of incubation, the droplets were reinjected into the sort chip to analyze the activation of reporter cells in the droplet, and approximately 9.5% of the reporter cells were activated. In contrast, when the anti-Her2 × anti-CD3 lentivirus-infected K562-Her2 cells were cocultured with reporter cells in the plate well, 72.7% of the reporter cells were activated after 16 hours of incubation (Fig. 3A). The divergence of reporter cell activation in the plate well and droplets demonstrates that antibodies secreted by cells in the droplet cannot diffuse between different droplets; thus, the system is suitable for screening a library. In addition, NucGreen Dead 488 was used to track the cell viability in droplets. Both K562-Her2 and Jurkat/pIL2-eGFP cells in the droplets exhibited a high viability of approximately 90% after 16 hours of incubation (fig. S3).

Screening anti-Her2 × anti-CD3 bispecific antibody using the function-based screening method

Because phage display technology can be used to screen an antibody library with much larger diversity than is possible in eukaryotic systems, we first selected Her2-binding antibodies from an antibody

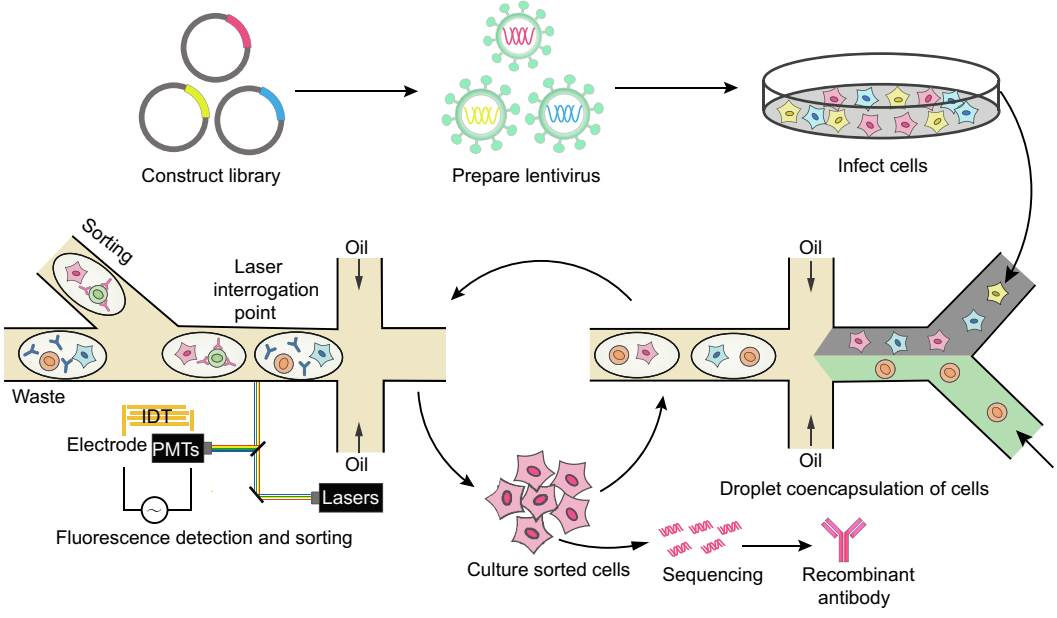

Fig. 1. Schematic overview of functional antibody screening using a droplet-based microfluidic system. The antibody genes were cloned into lentiviral vectors. Eukaryotic cells were infected with the lentiviral antibody library, and individual transduced cells were coencapsulated with the reporter cell into droplets using a microfluidic system. The resulting emulsion was incubated off-chip overnight and injected into the sorting chip. Droplets containing antibody-secreting cells and activated reporter cells were sorted. The sorted cells were cultured for the next round of selection. After multiple rounds of iteration, antibody genes were amplified from the sorted cells and analyzed by Sanger sequencing or next-generation sequencing. The enriched antibodies were synthesized, and recombinant antibodies were expressed and tested for function. PMTs, photomultiplier tubes. IDT, interdigital transducer.

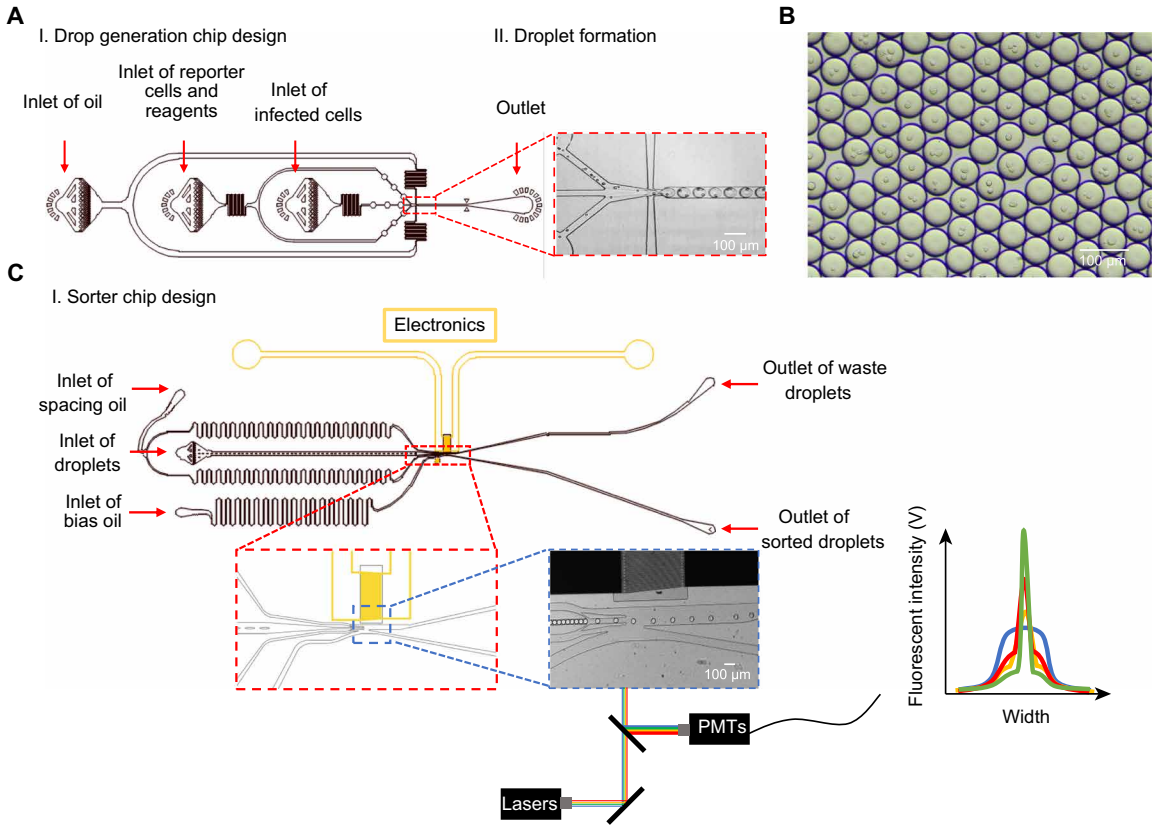

Fig. 2. Microfluidic chips. (**A**) The droplet generation chip is used to generate droplets to coencapsulate antibody-secreting cells with reporter cells. (**B**) Image of generated droplets. (**C**) The sorting chip is used to collect droplets based on the intensity of fluorescence. The functions of various inlets are indicated, and images of outlets for droplet generation and sorting are shown.

phage display library. We panned a naïve human single-chain Fv (scFv) library with a diversity of 10^{10} members against the Her2 protein. One round of panning was performed, and the scFv genes in phagemid were subcloned into a lentiviral vector that contained a fixed blinatumomab-derived anti-CD3 scFv gene to express anti-Her2 × antib-CD3 BiTE antibodies. The size of the combinatorial bispecific antibody library was approximately 10^5 members.

K562-Her2 cells were infected with the BiTE antibody lentivirus library at low MOI to ensure that most cells were infected with only one virus and thus produced a single type of bispecific antibody. Before cell encapsulation, K562-Her2 cells and Jurkat/pIL2-eGFP cells were stained with CellTrace Violet and Yellow dyes, respectively. The infected K562-Her2 cells were individually coencapsulated with Jurkat/pIL2-eGFP reporter cells into droplets, which were sorted after 16 hours of incubation (fig. S4). We first selected droplets for the presence of K562-Her2 and Jurkat/pIL2-eGFP cells based on the cell staining fluorescence signals. Then, we selected droplets if the reporter cell inside was activated on the basis of the GFP signal. Last, we selected droplets if the GFP signal was colocalized with the reporter cell staining signal. Eleven million droplets were imaged, approximately 0.26% of the droplets were sorted, and an image of representative sorted droplets is shown in Fig. 3B. The anti-Her2 scFv genes were amplified from the sorted cells and cloned into a mammalian expression plasmid. Twenty clones were selected for Sanger sequencing, and five bispecific antibodies appeared more than once. The purified bispecific antibodies were added to Jurkat/pIL2-eGFP reporter cells in coculture with K562-Her2. Three of the five antibodies (BiTE1, BiTE2, and BiTE3) activated the reporter cell in the presence of K562-Her2 (Fig. 3C). To assess the antitumor activity of BiTE1, we performed in vitro cytotoxicity assays by coculturing peripheral blood mononuclear cells (PBMCs) and HER2-expressing SK-BR-3 breast cancer cells. The results showed that lysis of SK-BR-3 cells only occurred when they were incubated with BiTE1, not with the control antibody anti-CD3 × anti-HEL (hen egg lysozyme) (Fig. 3D). Flow cytometry analysis of T cells in the coculture system showed that BiTE1 stimulated the expression of the activation marker CD69 on T cells (Fig. 3E). Moreover, BiTE1 induced dose-dependent increases in interferon-γ (IFN-γ) and interleukin-2 (IL-2) in the supernatants (Fig. 3, F and G). Overall, the results demonstrate that this technology allows combinatorial screening and profiling of large numbers of bispecific antibodies.

Discrimination of the strong and weak hits by the method

To validate the potential of the method to discriminate between strong and weak hits, trastuzumab-derived anti-Her2 × anti-CD3 positive control, BiTE1, and BiTE3 in descending order of potency were each cloned into lentiviruses. Cells infected with each of these bispecific antibodies encoding lentivirus were coencapsulated with the reporter cell, and droplets were analyzed for the activation of the reporter cell. The order of droplet intensity was as follows: trastuzumab-derived anti-Her2 × anti-CD3 positive control > BiTE1 ≈ BiTE3 (fig. S5). This work demonstrates the capability of the technology to

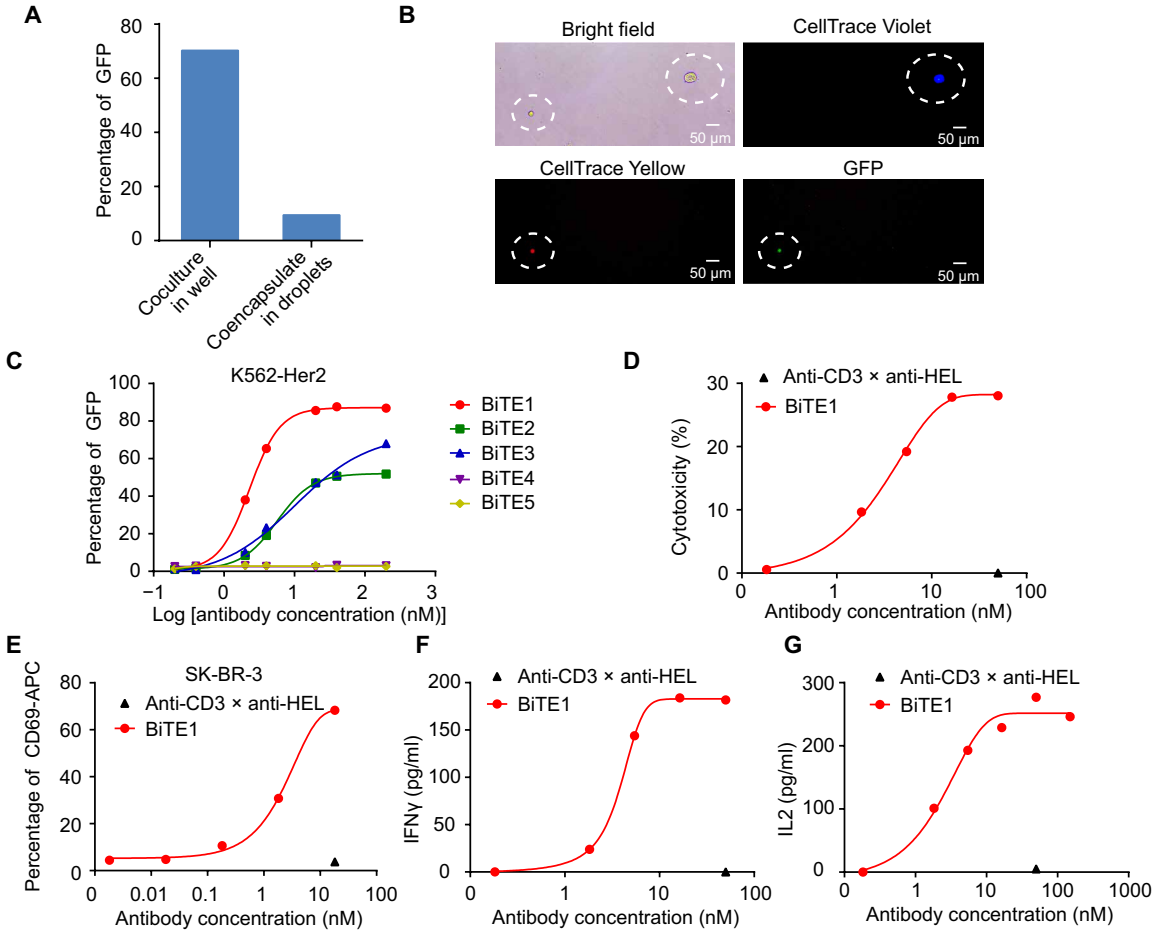

Fig. 3. Screening anti-Her2 × anti-CD3 BiTE antibody from a bispecific antibody library. (**A**) Activation of reporter cells in plate well–based or droplet-based cocultures. K562-Her2 cells expressing the anti-Her2 × anti-CD3 BiTE positive control were cocultured with Jurkat/pIL2-eGFP reporter cells in plate wells or individually coencapsulated with reporter cells. The activation of reporter cells under both conditions was compared. (**B**) Representative images of a sorted droplet. Antibody-secreting K562-Her2 cells and reporter cells were stained with CellTrace Violet and CellTrace Yellow dyes, respectively. K562-Her2 cells were individually coencapsulated with the reporter cell, and droplets containing activated reporter cells were sorted. (**C**) Activation of reporter cells by the identified antibodies. K562-Her2 cells were cocultured with reporter cells in the presence of the identified antibodies. Expression of GFP by the reporter cell was analyzed. (**D** to **G**) PBMC and tumor cell coculture assay. PBMCs and SK-BR-3 cells were cocultured in the presence of BiTE1 or control antibody. Tumor cell lysis was determined by measuring the release of lactic acid dehydrogenase (LDH) from tumor cells. (D) Expression of the activator marker CD69 on T cells was investigated (E), and levels of cell-secreted IFN-γ (F) and IL-2 (G) in the culture supernatant were measured by ELISA.

discriminate between weak and strong hits, which enables fast enrichment of high-potency hits using a more stringent gating strategy.

Proof-of-concept screening of CD40 agonists from a spike-in library

To further validate the utility of the function-based screening method, we sought to identify CD40 agonistic antibodies. CD40 is a promising drug target for cancer immune therapy (*5*). Activation of CD40 on antigen-presenting cells (APCs) results in improved antigen processing and presentation and cytokine release, which enhances the T cell response.

Human Jurkat T cells were engineered to express human CD40 and GFP controlled by nuclear factor κB (NF-κB) response elements. The reporter cell line expressed GFP when CD40 was activated (fig. S6). Human embryonic kidney (HEK) 293FT cells coexpressing red fluorescence protein (RFP) and the hexameric form of CD40L were used as positive controls (CD40L cells). HEK293FT cells coexpressing blue fluorescence protein (BFP) and HEL antibodies were used as negative controls (HEL cells). CD40L or HEL cells were coencapsulated with Jurkat/NF-κB-GFP-hCD40 reporter cells into droplets. After 16 hours of incubation, 24% of the droplets containing the CD40L cell and reporter cell exhibited a GFP fluorescence signal, while the HEL cell and reporter cell coencapsulating droplets exhibited a clean background of activation of the reporter cell (0.5%) (fig. S7).

Next, CD40L cells were spiked into a 10-fold excess of HEL cells. The mixture of CD40L cells and HEL cells was coencapsulated with Jurkat/NF-κB-GFP-hCD40 reporter cells with 0.5 protein-secreting cells per droplet. The droplets that contained activated reporter cells were sorted on the basis of the green fluorescence. Before sorting, only 1.24% of the mixed cell population were RFP positive, 16.79% of cells were BFP positive, and the remaining droplets were empty or contained only reporter cells; whereas after sorting, the percentage of droplets containing RFP-positive CD40L cells increased

to 51.94%, where 49.24% were RFP positive and 2.70% were RFP and BFP double positive (Fig. 4A). We also observed that most droplets contained both RFP-positive CD40L cells and GFP-positive reporter cells after sorting (Fig. 4B).

Screening CD40 agonist antibody using the function-based screening method

We first selected CD40-binding antibodies from an antibody library using phage display technology. The scFv genes in phagemid were subcloned into a lentiviral vector that contained the immunoglobulin G1 (IgG1) Fc gene to express scFv Fc fusion proteins. The library size was approximately 10^5. HEK293FT cells were infected with a lentivirus library at low MOI to ensure that most cells were infected with only one virus and produced one type of monoclonal antibody.

To screen CD40 agonist antibodies, antibody-producing cells were coencapsulated with CellTrace Yellow–prestained Jurkat/NF-κB-GFP-hCD40 reporter cells and DyLight 650–conjugated secondary antibodies in droplets. The reporter cells were also coencapsulated with soluble hexameric CD40L protein and anti-HEL antibody as positive and negative controls, respectively. Droplets of different populations (positive control, negative control, and the screening population) were coded by adding different concentrations of DY405. After 16 hours of incubation, the droplets were sorted on the basis of the following criteria (fig. S8). The droplets containing the screening population were gated on the basis of the intensity of DY405. The CellTrace Yellow fluorescence signal showed the presence of reporter cells in the droplet. The DyLight 650 fluorescence signal indicated binding of the secreting antibodies to CD40 on the surface of the reporter cell, and the GFP fluorescence signal indicated activation of the reporter cell (fig. S8). The droplets displayed different patterns of fluorescence signals (Fig. 5A and fig. S9). Thirteen million and 4.8 million droplets were imaged for the first and the second round of screening, respectively. Whereas only 0.29% of the droplets were DyLight 650 and GFP double positive for the first round of screening (among the droplets containing reporter cell signal), this value increased to 12.5% for the second round of screening (Fig. 5B). Droplets were imaged after sorting, and the number of DyLight 650 and GFP double-positive droplets was markedly increased (Fig. 5C).

The scFv genes were amplified from the cells after each round of sorting and subjected to third-generation sequencing. Circular consensus sequences (CCSs) from these reads were generated and filtered by quality, and full-length scFvs were identified in 44,084 reads. Considering the errors introduced by polymerase chain reaction (PCR) or sequencing, similar (at 95% similarity) scFv sequences were grouped into 561 scFv clusters, and consensus scFv sequences of each cluster were created. Comparison of the sequence frequency in each round revealed that some scFvs were enriched, while some scFvs were eliminated during selection (Fig. 5D). The frequency of scFv clusters C01, C03, C04, C05, and C06 was low before sorting and showed a roundwise increase during the selection process. In contrast, scFv cluster C02 was highly abundant before sorting, while its frequency was substantially reduced after selection (Fig. 5E).

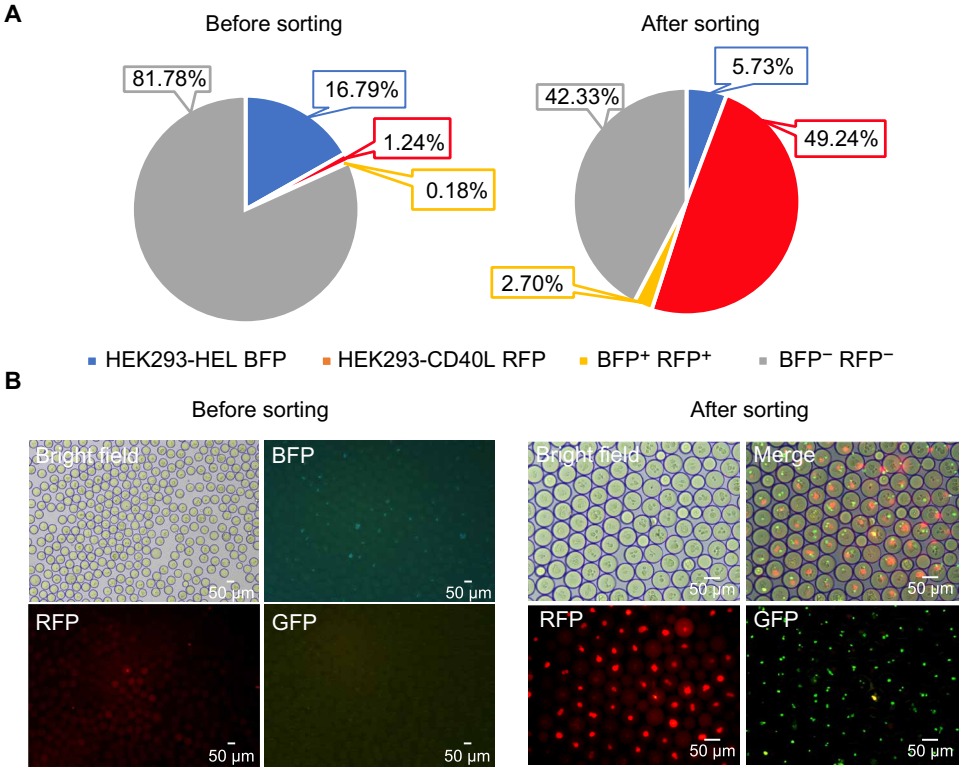

Fig. 4. Screening CD40 agonist from a spike-in library using a microfluidic system. (**A**) RFP-positive hexameric CD40L protein–secreting cells were spiked into a 10-fold excess of BFP-positive anti-HEL antibody–secreting cells, and the mixture of cells was coencapsulated with the reporter cells. After incubation, droplets containing activated reporter cells were sorted. The proportion of droplets containing RFP- or BFP-positive cells before and after sorting was analyzed. (**B**) Bright-field and fluorescence images of droplets before and after sorting.

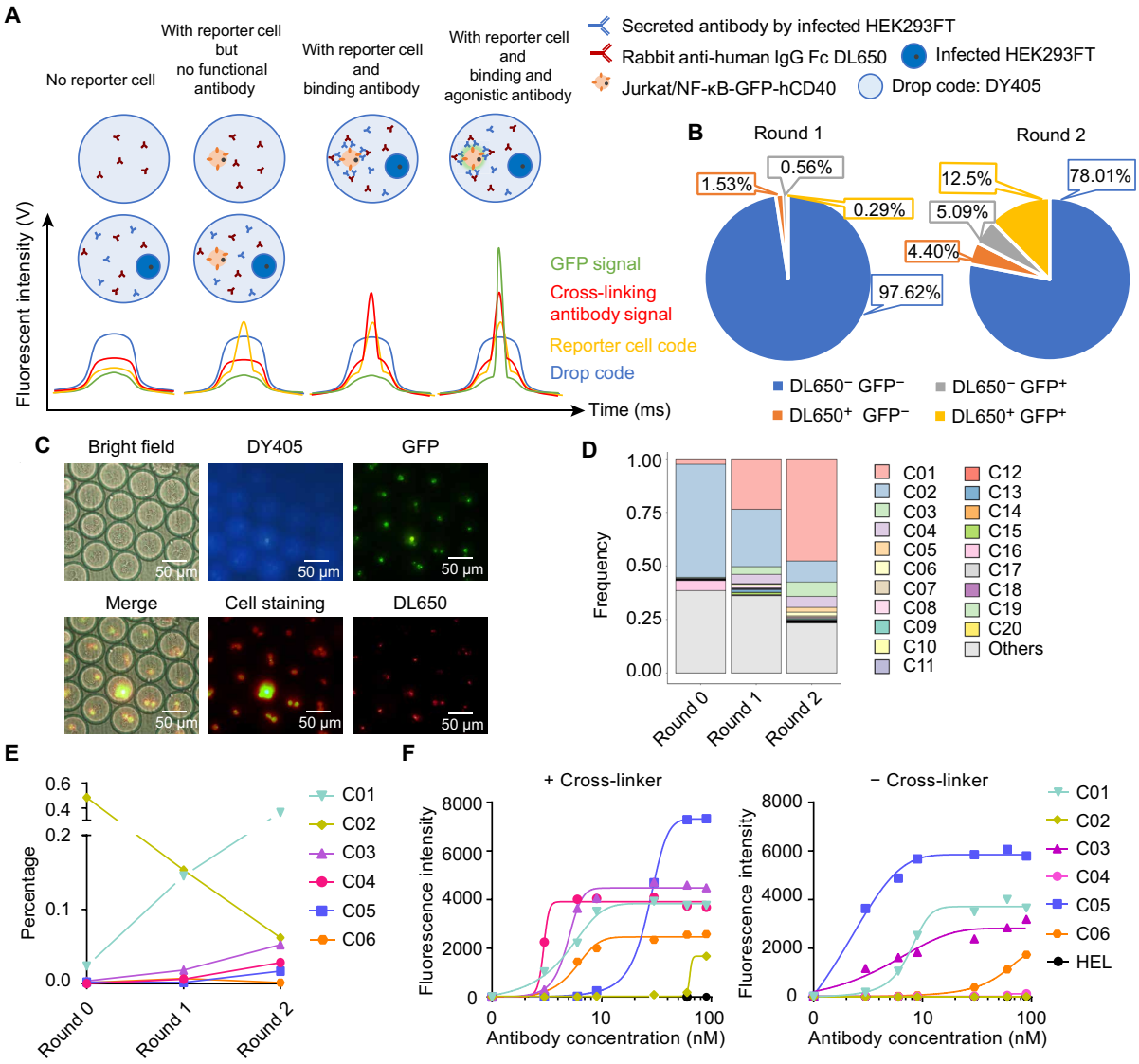

Fig. 5. Screening CD40 agonist antibody from a monoclonal antibody library. HEK293FT cells were infected with a lentivirus antibody library and individually coencapsulated with Jurkat/NF-κB-GFP-hCD40 reporter cells and fluorescence-labeled secondary antibodies in droplets. Droplets containing reporter cells activated by antibodies secreted by the coencapsulated antibody–expressing cells were sorted. The sorted cells were expanded for the second round of selection, and enriched antibodies were identified by next-generation sequencing. (**A**) Schematic of possible time traces. (**B**) Proportions of different types of droplets for each round of selection were analyzed. (**C**) Bright-field and fluorescence images of the sorted droplets after the second round of selection. (**D**) Bar plot for the top 20 scFv clusters and their frequencies during the selection process. (**E**) The change in frequencies of the selected antibodies during the selection process. (**F**) Agonist activity of the selected antibodies was determined using the CD40 reporter cell line in the presence or absence of the cross-linking secondary antibody.

The full-length IgG C01, C02, C03, C04, C05, and C06 genes were synthesized, and recombinant antibodies were expressed and purified. The activity of these antibodies was tested using the Jurkat/NF-κB-GFP-hCD40 reporter cell line. Reporter cells were stimulated with different concentrations of antibody in the presence or absence of the cross-linking secondary antibody. Antibodies C01, C03, C04, C05, and C06 activated the reporter cell line. The activity of C01, C03, and C05 was independent of cross-linking, while C04 and C06 activated the reporter cells in a cross-linking–dependent manner (Fig. 5F). We compared the signal intensities between Fc-dependent C04 and Fc-independent C01 in the droplet-based assay, and the results supported the differential Fc dependency of these hits (fig. S10). The activity of CD40 agonist antibodies independent of Fc receptor–mediated cross-linking might be disconcerting due to the potential for adverse events (*29*, *30*). Therefore, the cross-linking–dependent C04 antibody was chosen for further characterization.

Flow cytometry and surface plasmon resonance (SPR) results revealed that the C04 antibody bound to human, rhesus macaque, and cynomolgus monkey CD40 with similar affinity (fig. S11, A and B). In addition, enzyme-linked immunosorbent assay (ELISA) results confirmed that antibody C04 specifically bound to CD40 rather than other tumor necrosis factor (TNF) receptor superfamily members, such as TNF receptor superfamily member 18 (GITR), TNF

receptor superfamily member 4 (OX40), or TNF receptor superfamily member 9 (4-1BB) (fig. S11C).

Given that FcγRIIB expression on tumor-infiltrating myeloid cells is required for the agonistic activity of the cross-linking–dependent CD40 agonist antibodies, the FcγRIIB dependency of antibody C04 was confirmed. The Jurkat/NF-κB-GFP-hCD40 reporter can be stimulated by C04 in the presence of FcγRIIB-overexpressing cells. Results showed that the agonism of C04 was FcγRIIb dependent (Fig. 6A).

To investigate whether C04 promotes the activation of APCs, we stimulated human dendritic cells (DCs) and B cells isolated from PBMCs with C04 in the presence or absence of the cross-linking antibody. Flow cytometry analysis showed that C04 up-regulated the expression of the activation marker CD86 on DCs and B cells and that anti–Fc-mediated cross-linking further enhanced the maximum response of the antibody (Fig. 6B).

The immunostimulatory activity of antibody C04 was further assessed by the ovalbumin (OVA)–specific $CD8^+$ T cell response model in FcγR/CD40-humanized mice. Mice treated with the CD40 agonist antibody exhibited an increased number and percentage of OT-I cells among $CD8^+$ T cells compared to mice treated with the isotype antibody, demonstrating that C04 had a robust adjuvant effect (Fig. 6C).

In addition, the antitumor efficacy of C04 was assessed in syngeneic tumor models. When MC38 tumors were established (~100 mm^3), mice were treated with C04, CP-870,893 (Pfizer), or anti-HEL antibodies. C04 displayed comparable antitumor activity to CP-870,893, which is the most potent CD40 agonistic antibody among those studied in clinical trials. In addition, treatment with C04 caused

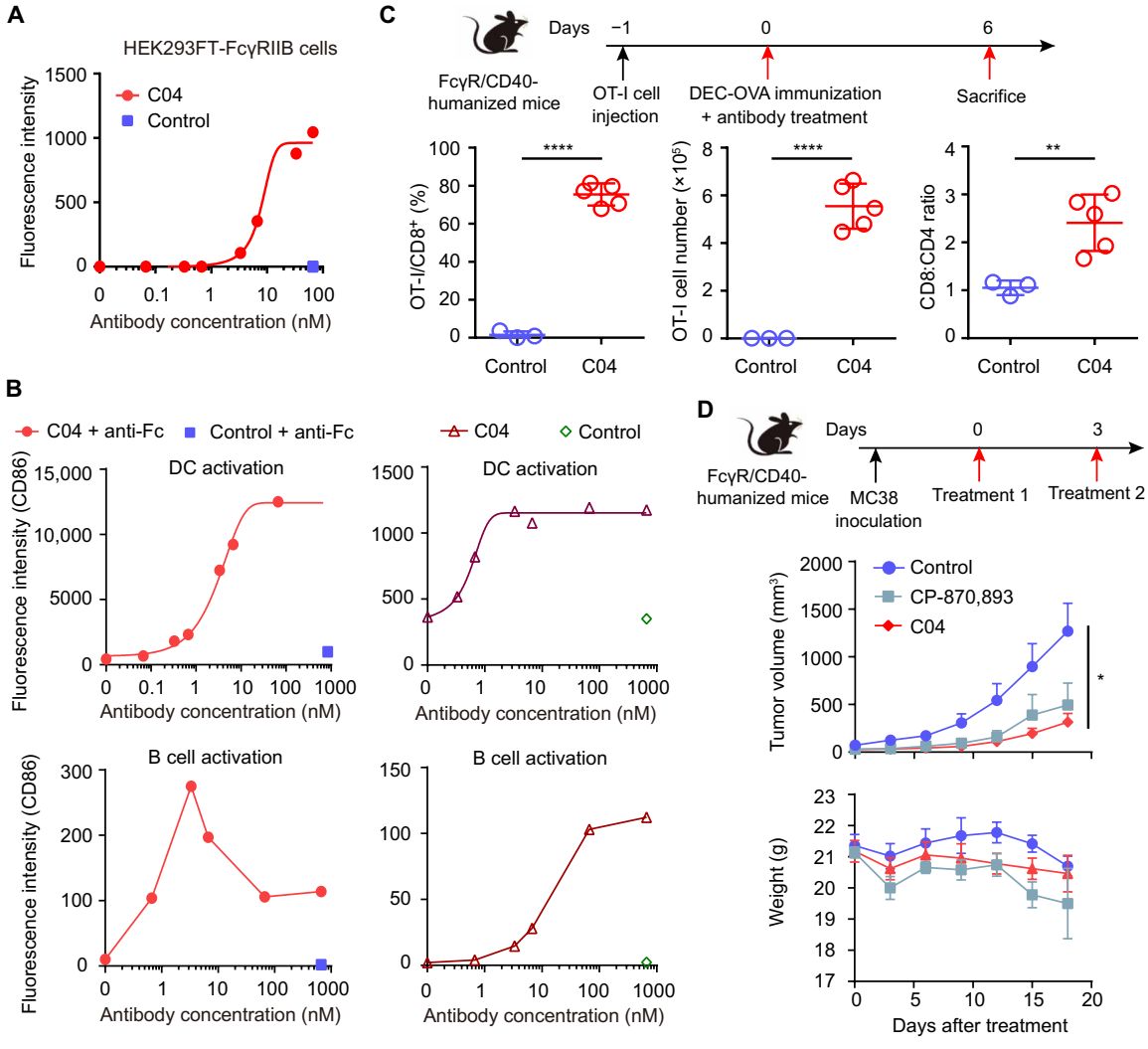

Fig. 6. Characterization of the identified CD40 agonist antibody. (**A**) The FcγRIIB dependency of antibody C04. Jurkat/NF-κB-GFP-hCD40 reporter cells were stimulated with C04 antibody or anti-HEL antibody in coculture with FcγRIIB-overexpressing HEK293FT cells. Activation of the reporter cell line was analyzed by flow cytometry. (**B**) Activation of DCs or B cells by C04. DCs or B cells isolated from a donor were stimulated by C04 in the presence (left) or absence (right) of the cross-linking secondary antibody. Expression of CD86 was analyzed by flow cytometry. (**C**) OVA-specific $CD8^+$ T cell response induced by C04 in FcγR/CD40-humanized mice. Transgenic mice were adoptively transferred with OVA-specific OT-I cells and treated with DEC-OVA, together with C04 or isotype control antibody. Mice were euthanized for the analysis of T cells. Each circle represents an individual mouse. (**D**) Antitumor effect of C04 in the syngeneic mouse model. FcγR/CD40-humanized mice were subcutaneously engrafted with MC38 tumor cells. When MC38 tumors were established (~100 mm^3), mice were treated with C04, CP-870,893, or isotype control antibody. Tumor volume and body weight were measured every 3 days until the end of the experiment. Data are represented as the means ± SEM. *$P < 0.05$, **$P < 0.01$, ****$P < 0.0001$.

relatively less body weight reduction than CP-870,893 treatment, suggesting that C04 has a favorable toxicity profile (Fig. 6D).

DISCUSSION

Here, we describe a droplet-based microfluidic platform for the functional screening of millions of antibodies. The platform shares some key features with the most efficient selection methods, such as phage display (*8*–*13*). First, the genotype and phenotype linkage was maintained throughout the whole process. Second, the product from one round can be directly amplified and used as the input in the next round of selection. Thus, multiple rounds of iteration allow the enrichment of rare hits. Compared to the conventional method of individually expressing and assaying thousands of antibodies, the throughput of this platform increased that limit to 10 million. This is especially useful for the development of next-generation cancer immunotherapies, such as agonist antibodies or bispecific antibodies, when simple binding assays may be inadequate. To demonstrate the usefulness of this platform, we first applied it to discover bispecific antibodies and agonist antibodies, whose development was limited by low-diversity and/or low-throughput and potentially biased screening.

Bispecific T or natural killer (NK) cell engagers (BiTEs or BiKEs) hold great promise for cancer treatment, and a growing number of BiTEs and BiKEs are making their way through various stages of development (*6*). To identify the optimal BiTE or BiKE, we constructed a bispecific antibody library to address the complexity of the array of tumor antigen–targeting antibodies. The large number of bispecific antibodies in a given library can exceed the throughput of existing methods. The described approach provides significant opportunities to screen unprecedented numbers of molecules of different formats and compositions, such as antibodies and nonantibody protein scaffolds (*31*). However, the method by itself cannot guarantee the generation of functional hits of high potency, and the successful isolation of potent antibodies also depends on the existence of such hits in the library. Similar to other in vitro display methods, the efficiency of drug discovery will scale with library size (*32*).

We performed a single round of screening to identify anti-Her2 × anti-CD3 antibodies. Such a single round could be potentially sufficient for some targets, but the false-positive rate could be high in certain screenings. A few reasons could contribute to the false-positive rate. First, the local concentration of antibody in the droplets is very high and may result in an increased tendency to form high–molecular weight aggregates and nonspecific activation of the reporter cell. Second, the gating strategy may not be stringent enough to exclude all false-positive events. As used in well-established methods, such as phage display, iterative rounds of screening may help to enrich the true hits and eliminate false-positive hits. In addition, more stringent gating strategies can be applied in screening.

Research into costimulatory receptor agonists has been reignited over the past decade due to substantial advances in the field of immunoncology. Costimulatory receptors are expressed on a number of immune cell types, including T cells, B cells, and NK cells as well as APCs, and engagement of these receptors promotes immune cell function, proliferation, and survival. Nevertheless, there are no general rules to guide the screening of agonist antibodies. For example, a panel of antibodies binds to the same or similar epitopes of the Fas receptor but results in different biological effects, with some acting as agonists and others as antagonists (*4*, *33*). The intrinsic complexity of agonist antibodies requires screening as many antibodies as possible. We used our unique platform to screen for CD40 agonist antibody and found a few potent CD40 agonist antibodies, most of which were too rare (<0.02% frequency) to be found using a conventional screening platform.

Our method can also be applied to high-throughput analysis of cell-cell interactions. For example, we can envision a scenario where DCs infected with a lentivirus library encoding neoantigens are coencapsulated with tumor-infiltrating T cells to map the pairs of cognate antigens and T cell receptors (TCRs) (*34*). This method can also be adapted to screen different types of molecules, such as cytokines (*35*–*37*). In addition to application in drug discovery, identification of intercellular signaling pathways has become an actively growing field. Combining our technology with the power of CRISPR-Cas9 library screening could enable the deciphering of cell-cell communications at scale (*38*–*40*). The innovative applications of this activity-based selection method have been limited only by the imagination of the users.

In summary, we developed a unique high-throughput platform for function-based screening of up to millions of antibodies. With the capability to screen millions of antibody-producing cells without any presumptions other than the key function used for screening, this may revolutionize next-generation cancer immunotherapy drug discovery and development as well as advance basic research involving cell-to-cell interactions.

MATERIALS AND METHODS

Cell culture

HEK293FT cells (Thermo Fisher Scientific, R70007) were cultured in Dulbecco's modified Eagle's medium (DMEM) (Thermo Fisher Scientific). Jurkat cells [American Type Culture Collection (ATCC), TIB-152] were cultured in RPMI 1640 medium (Thermo Fisher Scientific). SK-BR-3 cells (ATCC, HTB-30) were cultured in McCoy's 5A (modified) medium (Biological Industries). All the culture medium was supplemented with 10% fetal bovine serum (FBS; Biological Industries), 1× nonessential amino acids, penicillin (100 U/ml), streptomycin (100 μg/ml), and 12.5 mM Hepes (Thermo Fisher Scientific). HEK293F cells (Thermo Fisher Scientific, R79007) were suspended and cultured in FreeStyle 293 Expression Medium (Thermo Fisher Scientific). All cells were maintained in a CO_2 incubator at 37°C.

IL2 reporter cell line

Jurkat/pIL2-eGFP was developed to monitor the activation of T cells. The Jurkat cell line was transfected with a vector carrying the eGFP reporter gene under the control of the full-length IL-2 promoter (the region from −648 to −1 upstream of the translation initiation codon of IL2). After stimulation with anti-CD3 and anti-CD28 antibodies, cells expressing high levels of GFP were sorted into wells of a 96-well plate using fluorescence-activated cell sorter (FACS), and individual clones of the Jurkat/pIL2-eGFP cell line were characterized.

CD40 reporter cell line

Jurkat/NF-κB-GFP-hCD40 reporter cells were developed to monitor the activation of CD40. Jurkat cells were transfected with a vector carrying the eGFP reporter gene under the control of the NF-κB response element. After stimulation with TNFα (10 ng/ml; Sino

Biological), cells expressing a high level of eGFP were sorted by FACS, and the Jurkat/NF-κB-eGFP cell line was characterized. The resulting Jurkat/NF-κB-eGFP cell line was infected with lentivirus expressing full-length human CD40. After stimulation with 100 nM hexameric CD40L Fc fusion protein, individual cells with a high GFP signal level were sorted into wells of a 96-well plate by FACS, and individual clones of Jurkat/NF-κB-GFP-hCD40 cells were characterized.

Microfluidic chip fabrication

All microfluidic chips were fabricated in polydimethylsiloxane (PDMS) polymers (Sylgard 184 Elastomer Kit; Dow Corning Corp.) using standard soft lithography as previously described (*41*). Masters were made using one layer of SU-8 photoresist (MicroChem). The depth of the two devices is 40 ± 1 μm to allow the droplet to generate or flow in a monolayer format. Device i is composed of one oil inlet and two aqueous phase inlets where reporter cells, infected cells, and bioassay reagents are added. For device ii, PDMS is bound to a piezoelectric substrate (Y128-cut lithium niobate wafer), where a gold interdigital electrode is patterned with standard lift-off technology and aligned with the fluidic channel above. Microfluidic devices were treated before use with 1% (v/v) 1*H*,1*H*,2*H*,2*H*-perfluorodecyltrichlorosilane (Alfa Aesar) in Novec HFE7500 fluorinated oil (3M) to prevent droplets from wetting the channel walls.

Droplet production, collection, and incubation

Aqueous phases containing infected cells and reporter cells were coflowed and partitioned into droplets with hydrodynamic flow focusing in dripping mode on a microfluidic chip (Fig. 2A). The nozzle is 15 μm wide, 40 μm deep, and 10 μm long. The continuous phase was Novec HFE7500 fluorinated oil (3M) containing 2% (w/w) 008-FluoroSurfactant (RAN Biotechnologies). Pressure pumps (Fluigent) were used to generate monodispersed droplets of 100 ± 10 pl at 5000 Hz. The droplets were collected into a 10-ml tube and incubated at 37°C in 5% CO_2 to allow antibody secretion and subsequent activity to occur within each droplet before screening.

Microfluidic droplet screening and recovery

Droplet fluorescence analysis and sorting operations were performed on a dedicated droplet microfluidic station, similar to that described by Mazutis *et al.* (*15*). Pressure pumps (Fluigent) were used to inject the collected droplets into the sorter device (Fig. 2C) at a frequency of 1000 to 3000 Hz. The sorter device was mounted on an inverted microscope (Applied Scientific Instrumentation Microscope) equipped with a 940-nm light-emitting diode illumination source (Thorlabs, M940L3) and a fixed focus laser line (solid-state laser with a wavelength of 405, 488, 561, or 635 nm; Omicron) with photomultiplier tube bandpass filters of 440/40 to 25, 525/40 to 25, 593/46 to 25, and 708/75 to 25 nm (Hamamatsu).

The fluorescence of each droplet was measured as the droplet flowed past an observation constraint in the microfluidic channel where the laser line was positioned. The emitted fluorescence was detected with photomultiplier tubes, converted into corresponding signal output voltages, and recorded by the data acquisition card (FPGA PCIe-7842R). These voltages were then processed by the card and custom LabVIEW software to identify droplets according to their fluorescence intensity and size. These characteristics were used to determine whether each droplet should be sorted.

Droplets were sorted on the basis of the surface acoustic wave deflection as described by Franke *et al.* (*21*, *42*) with a gigahertz signal generator (Wavetek, model 3010). Sorted droplets were collected in a 1.5-ml Eppendorf tube. Cells were recovered by adding 100 μl of DMEM culture medium, followed by 100 μl of 1*H*,1*H*,2*H*,2*H*-perfluoro-1-octanol (Sigma-Aldrich, 37053), and then cells were pooled and centrifuged at 400*g* for 5 min at 4°C for subsequent steps, such as subculture or DNA sequencing.

Phage display

A human naïve scFv library was constructed using PBMCs from 30 healthy donors with standard protocols. The phage library was incubated with biotinylated CD40-Fc fusion protein or Her2 recombinant protein (ACROBiosystems) for 2 hours at room temperature, and the phage-antigen complex was captured by Dynabeads M280 (Life Technologies). Bound phages were eluted using glycine-HCl (pH 2.2) for 10 min at room temperature and neutralized with tris-HCl (pH 8.0) to adjust the pH to 7.5. The phagemid DNA was isolated using a plasmid miniprep kit (QIAGEN).

Lentivirus library construction

Both phagemids and the lentiviral vector pLV-ef1α-scFv-Fc were digested with the Sfi I enzyme. The lentiviral vector and scFv genes were isolated after electrophoresis. ScFv genes were ligated into a lentiviral vector. The product of the ligation reaction was transformed into XL1-Blue competent cells by the electroporation transformation technique, and most of the transformed bacteria were plated on LB agar plates. The remaining bacteria were serially diluted and plated to estimate the size of the library. The lentiviral plasmid was prepared using a plasmid midiprep kit (QIAGEN) for lentivirus preparation.

Lentivirus preparation

When cell confluence reached 80%, HEK293FT cells were transfected with the lentiviral backbone plasmid and packaging plasmids using polyethylenimine (PEI; Polysciences) transfection reagent. The medium was changed to fresh complete culture medium 6 hours after transfection. The supernatant containing lentivirus was harvested after 48 hours, centrifuged at 300*g* for 5 min at 4°C, and filtered through a 0.45-μm filter to remove cell debris. Viral titer was measured using a P24 ELISA kit (Clontech). The virus was aliquoted and stored at −80°C.

Function-based screening of anti-Her2 × anti-CD3 bispecific antibody using microfluidics

For aqueous phase 1, Jurkat/pIL2-eGFP reporter cells were washed with phosphate-buffered saline (PBS) and stained with 1 μM CellTrace Yellow dye (Thermo Fisher Scientific, C34573) for 10 min at 37°C. The stained Jurkat/pIL2-eGFP reporter cells were washed two times with RPMI 1640 and resuspended in cell culture medium (RPMI 1640, 5% FBS, 25 mM Hepes, and 0.1% Pluronic F-68) containing anti-CD28 antibody (1 μg/ml; Invitrogen), which was added here to enhance T cell activation (fig. S1).

For aqueous phase 2, stable Her2-expressing K562 cells were infected with a lentiviral antibody library. The resulting antibody-secreting K562-Her2 cells were washed with PBS and stained with 1 μM CellTrace Violet dye (Thermo Fisher Scientific, C34571) for 10 min at 37°C. The stained cells were washed twice with RPMI 1640 and resuspended in cell culture medium containing 200 nM DY647 (Dyomics, 647-00). K562-Her2 cells infected with positive control lentivirus were resuspended in cell culture medium containing 1500 nM DY647.

Aqueous phases 1 and 2 were injected into the droplet generation chip from different inlets and used as the dispersion phase. Novec HFE7500 fluorinated oil (3M) containing 2% (w/w) fluorosurfactant (RAN Biotechnologies) was used as the continuous phase to produce droplets with an average size of 100 pl. The flow rates of aqueous phase 1, aqueous phase 2, and oil phase were adjusted so that 1 reporter cell and 0.5 antibody-secreting cells were coencapsulated per droplet on average. During droplet production, the cell suspension was cooled using ice water to inhibit antibody secretion. The droplets were collected and incubated at 37°C for 16 hours.

The droplets were first gated to eliminate coalesced droplets and retain only droplets of the desired size. The positive control and the screening population droplets were distinguished on the basis of the different intensities of fluorescence of DY647. For the screening population, droplets were selected for the presence of Jurkat/pIL2-eGFP reporter cells based on CellTrace Yellow signal and K562-Her2 cells based on CellTrace Violet signal. FADS was performed to sort the droplets containing Jurkat/pIL2-eGFP emitting GFP fluorescence. Last, we gated and sorted the droplets with GFP signal colocalized with reporter cell staining signal but not with K562-Her2 signal.

The cells were recovered from the sorted droplets by adding 200 μl of RPMI 1640 medium supplemented with 10% FBS and 24% Nycodenz (Serva, 31000.01), followed by the addition of 50 μl of 1*H*,1*H*,2*H*,2*H*-perfluoro-1-octanol (Sigma-Aldrich, 370533). After mixing thoroughly and centrifuging at 300*g* for 5 min at 4°C, the aqueous layer was completely separated and washed with RPMI 1640 medium. The recovered cells were lysed, and antibody genes were amplified from the cells.

Anti-Her2 × anti-CD3 bispecific antibody in vitro experiment Jurkat/pIL2-eGFP reporter cell assay

To determine the activity of anti-Her2 × anti-CD3 antibody candidates, Jurkat/pIL2-eGFP reporter cells were stimulated with different concentrations of anti-Her2/anti-CD3 antibodies and anti-CD28 antibody (1 μg/ml) in the presence of K562 cells or K562-Her2 cells. After 16 hours of incubation, GFP expression in reporter cells was detected by flow cytometry.

Anti-Her2 × anti-CD3 bispecific antibody ex vivo assay

A total of 1×10^5 PBMC cells were cocultured with SK-BR-3 cells at a 1:1 ratio. Different concentrations of anti-Her2 × anti-CD3 antibody or control antibody together with anti-CD28 antibody (1 μg/ml) were added. After 48 hours of incubation, cells were collected and stained with anti–CD3-FITC (BioLegend, 300406) and anti–CD69-APC (BioLegend, 310910) for 30 min at 4°C. T cell activation was determined by flow cytometry. Flow cytometry results were analyzed with FlowJo X software.

The cell supernatant was collected to quantify cytokine release and cytotoxicity. IL-2 (BD, 550611) and IFN-γ (R&D Systems, VAL104) were measured with ELISA kits according to the manufacturer's instructions. Cytotoxicity was analyzed by measuring the levels of released lactate dehydrogenase (LDH) using the CytoTox 96 Non-radioactive Cytotoxicity Assay protocol (Promega).

Function-based screening of CD40 agonist antibodies using microfluidics

For aqueous phase 1, Jurkat/NF-κB-GFP-hCD40 reporter cells were washed with PBS and stained with 1 μM CellTrace Yellow dye for 10 min at 37°C. The stained Jurkat/NF-κB-GFP-hCD40 reporter cells were washed two times with DMEM and resuspended at 20 million cells/ml in cell culture medium (DMEM, 5% FBS, 25 mM Hepes, and 0.1% Pluronic F-68) containing 16.67 nM DyLight 650–conjugated goat anti-human Fc IgG (Abcam, ab98622) and 24% Nycodenz. The secondary antibody DyLight 650–conjugated goat anti-human Fc IgG was used to mimic the cross-linking action by the Fc receptor (*43*).

For aqueous phase 2, for the screening population, HEK293FT cells were infected with a lentiviral antibody library and resuspended in cell culture medium containing 500 nM DY405 (Dyomics, 405-00). For positive control droplets, HEK293FT cells were resuspended in cell culture medium containing soluble hexameric CD40L protein and 1500 nM DY405. For negative control droplets, HEK293FT cells were resuspended in cell culture medium containing anti-HEL antibody and 2500 nM DY405.

Aqueous phases 1 and 2 were injected into the droplet generation chip from different inlets and used as the dispersion phase. Novec HFE7500 fluorinated oil (3M) containing 2% (w/w) fluorosurfactant (RAN Biotechnologies, 008-FluoroSurfactant) was used as the continuous phase to produce droplets with an average size of 100 pl. The flow rates of aqueous phase 1, aqueous phase 2, and oil phase were adjusted so, on average, 1 reporter cell and 0.5 antibody-secreting cell were coencapsulated per droplet. During droplet production, the cell suspension was cooled using ice water to inhibit antibody secretion. The droplets were collected and incubated at 37°C for 16 hours.

The droplets were first gated to eliminate coalesced droplets and retain only droplets of the desired size. Negative control droplets, positive control droplets, and screening droplets were distinguished on the basis of the different intensities of blue fluorescence of DY405. For the screening population, droplets were selected for the presence of Jurkat/NF-κB-GFP-hCD40 reporter cells in the droplet based on the yellow fluorescence of CellTrace Yellow dye. Last, FADS was performed to sort droplets containing Jurkat/NF-κB-GFP-hCD40 emitting DyLight 650 and GFP fluorescence. The cells were recovered from the sorted droplets by adding 200 μl of DMEM supplemented with 10% FBS and 24% Nycodenz, followed by adding 50 μl of 1*H*,1*H*,2*H*,2*H*-perfluoro-1-octanol (Sigma-Aldrich, 370533). After mixing thoroughly and centrifuging at 300*g* for 5 min at 4°C, the aqueous layer was completely separated and washed with DMEM. The cells were resuspended in DMEM containing 10% FBS and 1% penicillin and streptomycin and then cultured for 1 to 2 weeks.

Bioinformatic analysis of the PacBio sequencing results

A single-molecule real-time (SMRT) sequencing platform (Pacific Biosciences) generated long sequencing reads with an average read length of ~20 kb, which could sequence a scFv (subreads) more than 10 times. The circular consensus sequencing program from PacBio SMRT portal software (version 4.1.0) can take multiple subreads of the same SMRTbell sequence and combine them, using a statistical model, to produce one high-quality CCS. After CCS from long sequencing reads was generated, scFv flanking sequences were trimmed, scFv DNA sequences were translated into proteins using the CLC Genomics Workbench (version 11.0.1), and CDR1 to CDR3 regions for heavy and light chains were identified using IgBLAST (version 1.15.0). CD-hit (version 4.8.1) was used to group scFvs with a protein similarity of 95%. The frequency of scFvs for each round was calculated in the Java program. ScFvs that appeared in only one sample were removed because they were likely PCR

artifact products. The bar plot was drawn using the R package ggplot2 (version 3.2.1).

Protein expression and purification of full-length IgG

Equal amounts of the heavy chain and light chain expression plasmids were cotransfected into HEK293F cells. Five days after transfection, cells were centrifuged at 3000 rpm for 10 min at 4°C, and supernatants were harvested and passed through a 0.45-μm filter. Antibodies were purified with a HiTrap Protein A column (GE) using an ÄKTA purifier chromatography system.

CD40 in vitro experiment

Species cross-reactivity of antibody

Cross-reactivity of C04 was assessed by flow cytometry analysis. Briefly, HEK293FT cells were transiently transfected with human CD40 (hCD40)– or rhesus macaque CD40 (rCD40)–expressing vector using PEI. After 48 hours, HEK293FT-hCD40 or HEK293FT-rCD40 cells were incubated with different concentrations of antibody for 30 min at room temperature. Then, cells were stained with Alexa Fluor 488–conjugated goat anti-human Fc (Life Technologies) at room temperature for 30 min and analyzed by flow cytometry. The fluorescence intensity is equal to the percentage of GFP-positive cells multiplied by the median fluorescence intensity (MFI). The fluorescence intensity was plotted against the antibody concentrations using GraphPad Prism software.

SPR analysis

SPR experiments were performed with a Biacore T200 SPR system (GE Healthcare). In brief, experiments were performed at 20°C in HBS-P$^+$ buffer [0.01 M Hepes, 0.15 M NaCl, and 0.05% (v/v) Surfactant P20]. Anti-his antibody was immobilized on a Series S CM5 chip by amine coupling, and his-tagged cynomolgus monkey CD40 was captured by immobilized anti-his antibody at a flow rate of 10 μl/min for 60 s. Twofold serially diluted CD40 antibodies were injected through flow cells for 120 s followed by a 130-s dissociation phase at a flow rate of 30 μl/min. Before the next assay cycle, the sensor surface was regenerated with glycine-HCl (pH 1.5) for 30 s at a flow rate of 30 μl/min. Background binding to blank immobilized flow cells was subtracted, and equilibrium dissociation constant (K_D) values were calculated using the 1:1 binding kinetics model built in Biacore T200 Evaluation Software (version 3.2).

CD40 antibody selectivity

Human CD40 (ACROBiosystems), GITR (ACROBiosystems), OX40 (ACROBiosystems), 4-1BB (ACROBiosystems), or bovine serum albumin (BSA) (Solarbio) was plated onto a microtiter plate at 4°C overnight. The coated wells were blocked with 0.5% BSA in PBS at 37°C for 1 hour. Serially diluted antibodies were added and incubated at 37°C for 1 hour and washed eight times, followed by the addition of goat anti-human IgG–horseradish peroxidase (SouthernBiotech) and incubation at 37°C for 30 min. After eight washes, 2,2'-azinobis [3-ethylbenzthiazoline-6-sulfonic acid] diammonium salt (ABTS) substrate solution (Thermo Fisher Scientific) was added, and the optical density at 405 nm was measured with a plate reader.

Jurkat/NF-κB-GFP-hCD40 reporter cell assays

For CD40 agonist activity detection, Jurkat/NF-κB-GFP-hCD40 reporter cells were incubated with different concentrations of CD40 agonist antibodies with or without goat anti-human Fc antibody (SouthernBiotech) for 24 hours. GFP expression was detected by flow cytometry.

For the FcγRIIB dependency experiment, HEK293FT cells were transiently transfected with the FcγRIIB-expressing vector using PEI. After 36 hours, HEK293FT-FcγRIIB cells were plated in 48-well plates and cultured overnight at 37°C. Then, Jurkat/NF-κB-GFP-hCD40 reporter cells and different concentrations of C04 or anti-HEL were cocultured with HEK293FT-FcγRIIB cells for 24 hours. GFP expression was detected by flow cytometry.

For data analysis of Jurkat/NF-κB-GFP-hCD40 reporter cell assays, flow cytometry results were analyzed with FlowJo X software, and the fluorescence intensity was equal to the percentage of GFP-positive cells multiplied by MFI. The fluorescence intensity of cells was plotted against the antibody concentrations using GraphPad Prism software.

CD40 ex vivo experiment

Following thawing and recovery of human PBMCs, monocytes were selected by adhering to plastic and then cultured for 8 days in RPMI containing 10% FBS (Gibco), granulocyte-macrophage colony-stimulating factor (100 ng/ml; R&D Systems), and IL-4 (10 ng/ml; R&D Systems). Suspended cells were harvested and confirmed to be DCs by CD11c expression.

B cells were isolated from PBMCs by magnetic selection using CD19 beads (Miltenyi). A total of 1×10^5 DCs or B cells were incubated with different concentrations of C04 with or without goat anti-human Fc antibody (SouthernBiotech) for 48 hours. Upregulation of the activation marker CD86 was analyzed by flow cytometry (BioLegend). Flow cytometry results were analyzed with FlowJo X software. The MFI of cells was plotted against the antibody concentrations using GraphPad Prism software.

CD40 in vivo experiment

FcγR/CD40-humanized mice have been described previously and were provided by J. Ravetch (Rockefeller University). Mice were bred and maintained in a specific pathogen–free environment at the Department of Laboratory of Animal Science, Shanghai Jiao Tong University School of Medicine (SJTUSM). All animal care and study were performed in compliance with institutional and National Institutes of Health guidelines and were approved by the SJTUSM Institutional Animal Care and Use Committee (protocol registry number: A-2015-014).

OVA-specific CD8$^+$ T cell response model

FcγR/CD40-humanized mice were adoptively transferred with CD45.1$^+$ splenic OT-I cells (2×10^6 cells in 200 μl of PBS per mouse) via tail vein injection 1 day before immunization with 2 μg of CD205 (DEC)-OVA antibody in the presence of the CD40 agonist antibody or the isotype control by intraperitoneal injection. On day 6, spleen cells were harvested. After red blood cell lysis, the single-cell suspension was stained with anti-CD4 (clone RM4-5), anti-CD8 (clone 53-6.7), anti-CD45.1 (A20), and anti–TCR-Vα2 (B20.1) to quantify OVA-specific OT-I CD8$^+$ T cells. OT-I CD8$^+$ T cells were defined as CD45.1$^+$CD8$^+$TCR-Vα2$^+$ cells.

Syngeneic mouse model

FcγR/CD40-humanized mice were subcutaneously inoculated with 2×10^6 MC38 cells. When tumor volumes reached 50 to 100 mm^3, mice were randomly assigned to different groups ($n = 5$). MC38-bearing FcγR/CD40-humanized mice were intraperitoneally treated with C04, CP-870,893, or anti-HEL (3 mg/kg, q3d × 2). Tumor growth was monitored every 3 days by measuring the length (L) and width (W) with calipers, and tumor volume was calculated using the formula $(L \times W^2)/2$.

SUPPLEMENTARY MATERIALS

Supplementary material for this article is available at http://advances.sciencemag.org/cgi/content/full/7/24/eabe3839/DC1

View/request a protocol for this paper from *Bio-protocol*.

REFERENCES AND NOTES

1. L. P. Andrews, H. Yano, D. A. A. Vignali, Inhibitory receptors and ligands beyond PD-1, PD-L1 and CTLA-4: Breakthroughs or backups. *Nat. Immunol.* **20**, 1425–1434 (2019).
2. J. Tang, J. X. Yu, V. M. Hubbard-Lucey, S. T. Neftelinov, J. P. Hodge, Y. Lin, Trial watch: The clinical trial landscape for PD1/PDL1 immune checkpoint inhibitors. *Nat. Rev. Drug Discov.* **17**, 854–855 (2018).
3. A. Hoos, Development of immuno-oncology drugs - from CTLA4 to PD1 to the next generations. *Nat. Rev. Drug Discov.* **15**, 235–247 (2016).
4. P. A. Mayes, K. W. Hance, A. Hoos, The promise and challenges of immune agonist antibody development in cancer. *Nat. Rev. Drug Discov.* **17**, 509–527 (2018).
5. R. H. Vonderheide, CD40 agonist antibodies in cancer immunotherapy. *Annu. Rev. Med.* **71**, 47–58 (2020).
6. A. F. Labrijn, M. L. Janmaat, J. M. Reichert, P. W. H. I. Parren, Bispecific antibodies: A mechanistic review of the pipeline. *Nat. Rev. Drug Discov.* **18**, 585–608 (2019).
7. H. Li, P. Er Saw, E. Song, Challenges and strategies for next-generation bispecific antibody-based antitumor therapeutics. *Cell. Mol. Immunol.* **17**, 451–461 (2020).
8. G. P. Smith, Phage display: Simple evolution in a petri dish (Nobel lecture). *Angew. Chem. Int. Ed. Engl.* **58**, 14428–14437 (2019).
9. R. A. Lerner, Manufacturing immunity to disease in a test tube: The magic bullet realized. *Angew. Chem. Int. Ed. Engl.* **45**, 8106–8125 (2006).
10. A. R. Bradbury, S. Sidhu, S. Dübel, J. McCafferty, Beyond natural antibodies: The power of in vitro display technologies. *Nat. Biotechnol.* **29**, 245–254 (2011).
11. P. Amstutz, P. Forrer, C. Zahnd, A. Pluckthun, In vitro display technologies: Novel developments and applications. *Curr. Opin. Biotechnol.* **12**, 400–405 (2001).
12. E. T. Boder, K. D. Wittrup, Yeast surface display for screening combinatorial polypeptide libraries. *Nat. Biotechnol.* **15**, 553–557 (1997).
13. G. Georgiou, C. Stathopoulos, P. S. Daugherty, A. R. Nayak, B. L. Iverson, R. C. Iii, Display of heterologous proteins on the surface of microorganisms: From the screening of combinatorial libraries to live recombinant vaccines. *Nat. Biotechnol.* **15**, 29–34 (1997).
14. S. L. Anna, N. Bontoux, H. A. Stone, Formation of dispersions using "flow focusing" in microchannels. *Appl. Phys. Lett.* **82**, 364–366 (2003).
15. L. Mazutis, J. Gilbert, W. L. Ung, D. A. Weitz, A. D. Griffiths, J. A. Heyman, Single-cell analysis and sorting using droplet-based microfluidics. *Nat. Protoc.* **8**, 870–891 (2013).
16. N. Shembekar, C. Chaipan, R. Utharala, C. A. Merten, Droplet-based microfluidics in drug discovery, transcriptomics and high-throughput molecular genetics. *Lab Chip* **16**, 1314–1331 (2016).
17. G. Georgiou, G. C. Ippolito, J. Beausang, C. E. Busse, H. Wardemann, S. R. Quake, The promise and challenge of high-throughput sequencing of the antibody repertoire. *Nat. Biotechnol.* **32**, 158–168 (2014).
18. B. El Debs, R. Utharala, I. V. Balyasnikova, A. D. Griffiths, C. A. Merten, Functional single-cell hybridoma screening using droplet-based microfluidics. *Proc. Natl. Acad. Sci. U.S.A.* **109**, 11570–11575 (2012).
19. N. Shembekar, H. Hu, D. Eustace, C. A. Merten, Single-cell droplet microfluidic screening for antibodies specifically binding to target cells. *Cell Rep.* **22**, 2206–2215 (2018).
20. K. Eyer, R. C. L. Doineau, C. E. Castrillon, L. Briseño-Roa, V. Menrath, G. Mottet, P. England, A. Godina, E. Brient-Litzler, C. Nizak, A. Jensen, A. D. Griffiths, J. Bibette, P. Bruhns, J. Baudry, Single-cell deep phenotyping of IgG-secreting cells for high-resolution immune monitoring. *Nat. Biotechnol.* **35**, 977–982 (2017).
21. A. Gérard, A. Woolfe, G. Mottet, M. Reichen, C. Castrillon, V. Menrath, S. Ellouze, A. Poitou, R. Doineau, L. Briseno-Roa, P. Canales-Herrerias, P. Mary, G. Rose, C. Ortega, M. Delincé, S. Essono, B. Jia, B. Iannascoli, O. R.-L. Goff, R. Kumar, S. N. Stewart, Y. Pousse, B. Shen, K. Grosselin, B. Saudemont, A. Sautel-Caillé, A. Godina, S. M. Namara, K. Eyer, G. A. Millot, J. Baudry, P. England, C. Nizak, A. Jensen, A. D. Griffiths, P. Bruhns, C. Brenan, High-throughput single-cell activity-based screening and sequencing of antibodies using droplet microfluidics. *Nat. Biotechnol.* **38**, 715–721 (2020).
22. H. Zhang, E. Sturchler, J. Zhu, A. Nieto, P. A. Cistrone, J. Xie, L. He, K. Yea, T. Jones, R. Turn, P. S. Di Stefano, P. R. Griffin, P. E. Dawson, P. H. McDonald, R. A. Lerner, Autocrine selection of a GLP-1R G-protein biased agonist with potent antidiabetic effects. *Nat. Commun.* **6**, 8918 (2015).
23. H. Zhang, I. A. Wilson, R. A. Lerner, Selection of antibodies that regulate phenotype from intracellular combinatorial antibody libraries. *Proc. Natl. Acad. Sci. U.S.A.* **109**, 15728–15733 (2012).
24. A. V. Stepanov, O. V. Markov, I. V. Chernikov, D. V. Gladkikh, H. Zhang, T. Jones, A. V. Sen'kova, E. L. Chernolovskaya, M. A. Zenkova, R. S. Kalinin, M. P. Rubtsova, A. N. Meleshko, D. D. Genkin, A. A. Belogurov Jr., J. Xie, A. G. Gabibov, R. A. Lerner, Autocrine-based selection of ligands for personalized CAR-T therapy of lymphoma. *Sci. Adv.* **4**, eaau4580 (2018).
25. J. W. Blanchard, J. Xie, N. El-Mecharrafie, S. Gross, S. Lee, R. A. Lerner, K. K. Baldwin, Replacing reprogramming factors with antibodies selected from combinatorial antibody libraries. *Nat. Biotechnol.* **35**, 960–968 (2017).
26. K. Yea, J. Xie, H. Zhang, W. Zhang, R. A. Lerner, Selection of multiple agonist antibodies from intracellular combinatorial libraries reveals that cellular receptors are functionally pleiotropic. *Curr. Opin. Chem. Biol.* **26**, 1–7 (2015).
27. L. Schmid, D. A. Weitz, T. Franke, Sorting drops and cells with acoustics: Acoustic microfluidic fluorescence-activated cell sorter. *Lab Chip* **14**, 3710–3718 (2014).
28. R. Lutterbuese, T. Raum, R. Kischel, P. Hoffmann, S. Mangold, B. Rattel, M. Friedrich, O. Thomas, G. Lorenczewski, D. Rau, E. Schaller, I. Herrmann, A. Wolf, T. Urbig, P. A. Baeuerle, P. Kufer, T cell-engaging BiTE antibodies specific for EGFR potently eliminate KRAS- and BRAF-mutated colorectal cancer cells. *Proc. Natl. Acad. Sci. U.S.A.* **107**, 12605–12610 (2010).
29. D. Chen, Y. Zhao, M. Li, H. Shang, N. Li, F. Li, W. Wang, Y. Wang, R. Jin, S. Liu, X. Li, S. Gao, Y. Tian, R. Li, H. Li, Y. Zhang, M. Du, Y. Cao, Y. Zhang, X. Li, Y. Huang, L. A. Hu, F. Li, H. Zhang, A general Fc engineering platform for the next generation of antibody therapeutics. *Theranostics* **11**, 1901–1917 (2021).
30. F. Li, J. V. Ravetch, Inhibitory Fcγ receptor engagement drives adjuvant and anti-tumor activities of agonistic CD40 antibodies. *Science* **333**, 1030–1034 (2011).
31. R. Vazquez-Lombardi, T. G. Phan, C. Zimmermann, D. Lowe, L. Jermutus, D. Christ, Challenges and opportunities for non-antibody scaffold drugs. *Drug Discov. Today* **20**, 1271–1283 (2015).
32. R. A. Lerner, S. Brenner, DNA-encoded compound libraries as open source: A powerful pathway to new drugs. *Angew. Chem. Int. Ed. Engl.* **56**, 1164–1165 (2017).
33. M. Chodorge, S. Zuger, C. Stirnimann, C. Briand, L. Jermutus, M. G. Grutter, R. R. Minter, A series of Fas receptor agonist antibodies that demonstrate an inverse correlation between affinity and potency. *Cell Death Differ.* **19**, 1187–1195 (2012).
34. T. Kula, M. H. Dezfulian, C. I. Wang, N. S. Abdelfattah, Z. C. Hartman, K. W. Wucherpfennig, H. K. Lyerly, S. J. Elledge, T-Scan: A genome-wide method for the systematic discovery of T cell epitopes. *Cell* **178**, 1016–1028.e13 (2019).
35. J. B. Spangler, I. Moraga, J. L. Mendoza, K. C. Garcia, Insights into cytokine-receptor interactions from cytokine engineering. *Annu. Rev. Immunol.* **33**, 139–167 (2015).
36. J. T. Sockolosky, E. Trotta, G. Parisi, L. Picton, L. L. Su, A. C. Le, A. Chhabra, S. L. Silveria, B. M. George, I. C. King, M. R. Tiffany, K. Jude, L. V. Sibener, D. Baker, J. A. Shizuru, A. Ribas, J. A. Bluestone, K. C. Garcia, Selective targeting of engineered T cells using orthogonal IL-2 cytokine-receptor complexes. *Science* **359**, 1037–1042 (2018).
37. P. N. Kelly, Engineering cytokine-receptor pairs. *Science* **359**, 1004–1006 (2018).
38. L. Cong, F. A. Ran, D. Cox, S. Lin, R. Barretto, N. Habib, P. D. Hsu, X. Wu, W. Jiang, L. A. Marraffini, F. Zhang, Multiplex genome engineering using CRISPR/Cas systems. *Science* **339**, 819–823 (2013).
39. P. Mali, L. Yang, K. M. Esvelt, J. Aach, M. Guell, J. E. DiCarlo, J. E. Norville, G. M. Church, RNA-guided human genome engineering via Cas9. *Science* **339**, 823–826 (2013).
40. L. S. Qi, M. H. Larson, L. A. Gilbert, J. A. Doudna, J. S. Weissman, A. P. Arkin, W. A. Lim, Repurposing CRISPR as an RNA-guided platform for sequence-specific control of gene expression. *Cell* **152**, 1173–1183 (2013).
41. J. C. McDonald, G. M. Whitesides, Poly(dimethylsiloxane) as a material for fabricating microfluidic devices. *Acc. Chem. Res.* **35**, 491–499 (2002).
42. T. Franke, S. Braunmuller, L. Schmid, A. Wixforth, D. A. Weitz, Surface acoustic wave actuated cell sorting (SAWACS). *Lab Chip* **10**, 789–794 (2010).
43. S. M. Mangsbo, S. Broos, E. Fletcher, N. Veitonmaki, C. Furebring, E. Dahlen, P. Norlen, M. Lindstedt, T. H. Totterman, P. Ellmark, The human agonistic CD40 antibody ADC-1013 eradicates bladder tumors and generates T-cell-dependent tumor immunity. *Clin. Cancer Res.* **21**, 1115–1126 (2015).

Acknowledgments

Funding: This work was supported by the National Key Research and Development plan of China (grant number 2017YFA0504801), the National Natural Science Foundation of China (grant number 81872787), China Postdoctoral Science Foundation (grant number 2020M670625), the Fundamental Research Funds for the Central Universities, Nankai University (grant numbers ZB19100123 and 63191212), the Natural Science Foundation of Tianjin (grant number 19JCZDJC32900), the Key Laboratory of Immune Microenvironment and Disease open funding (grant number 20180102), Shanghai Municipal Science and Technology Commission (project no. 19431902900), and the National Key Research and Development plan of China (grant number 2018YFE0200401). F.L. and Y.Z. are also supported by the Innovative Research Team of High-level Local Universities in Shanghai (SSMU-2DCX20180100) and Shanghai Science and Technology Commission Projects (grant numbers 18140902600, 19431902900). The work was also sponsored by HiFiBiO Therapeutic funding. **Author contributions:** H.Z. designed all the experiments. Y.W., R.J., B.S., W.W., Y.Z., M.H., P.F., S.W., P. Mary, N.L., R.W., P. Ma, and R.L. performed the experiments. H.Zho., Y.W., B.S., H.Zha., Y.T.,

L.S., F.L., and Y.C. analyzed all the data and wrote the manuscript with the input of all authors.
Competing interests: Y.W., R.J., H.Z., B.S., M.H., and L.S. are inventors on a pending patent (Functional Screening Using Droplet-based Microfluidics) related to this work filed by HiFiBiO (Shanghai) Limited and Nankai University, serial no. PCT/CN2020/110616, filed 21 August 2020. All inventors of the patent are disclosed, and no other authors on this paper are also the inventors on the patent. The authors declare that they have no other competing interests.
Data and materials availability: All data needed to evaluate the conclusions in the paper are present in the paper and/or the Supplementary Materials. The tabulated underlying data for indicated figures are included in the attached CSV file. Additional data related to this paper may be requested from the authors.

Submitted 19 August 2020
Accepted 23 April 2021
Published 11 June 2021
10.1126/sciadv.abe3839

Citation: Y. Wang, R. Jin, B. Shen, N. Li, H. Zhou, W. Wang, Y. Zhao, M. Huang, P. Fang, S. Wang, P. Mary, R. Wang, P. Ma, R. Li, Y. Tian, Y. Cao, F. Li, L. Schweizer, H. Zhang, High-throughput functional screening for next-generation cancer immunotherapy using droplet-based microfluidics. *Sci. Adv.* **7**, eabe3839 (2021).

ScienceAdvances

High-throughput functional screening for next-generation cancer immunotherapy using droplet-based microfluidics

Yuan Wang, Ruina Jin, Bingqing Shen, Na Li, He Zhou, Wei Wang, Yingjie Zhao, Mengshi Huang, Pan Fang, Shanshan Wang, Pascaline Mary, Ruikun Wang, Peixiang Ma, Ruonan Li, Yujie Tian, Youjia Cao, Fubin Li, Liang Schweizer, and Hongkai Zhang

Sci. Adv., **7** (24), eabe3839.
DOI: 10.1126/sciadv.abe3839

Science Advances (ISSN 2375-2548) is published by the American Association for the Advancement of Science. 1200 New York Avenue NW, Washington, DC 20005. The title *Science Advances* is a registered trademark of AAAS.